Platelets drive immune suppression and glioblastoma growth in a sex-dependent manner via PAR4 signaling

Anthony R. Sloan[1,2] George Bukenya[1], Anu Aggarwal[1], Juyeun Lee[1,2], Daniel Rosaff[3,4], Tyler J. Alban[5,6], Ivan Juric[5,6], Daniel J. Silver[1,2,5], Liza Tack[1], Tanvi Navadgi[1], Natalie Reitz[1], Gavin P. Tannish[1], Xueer Yuan[1], Jesse Coker[2,5], Alliefair Scalise[1,7,8], Bhairavi Rajasekar[1,7,8], Alex Vincenti[1], Erin Mulkearns-Hubert[1,2,5], Craig M. Horbsinki[9], Andrew E. Sloan[10], Christopher G. Hubert[2,11], Jinquin Luo[12], Joshua B. Rubin[13,14], Evi X. Stavrou[15,16], Falk W. Lohoff[3,4], Marvin T. Nieman[17], Naseer Sangwan[1], Timothy A. Chan[2,6,18,19], Alok A. Khorana[1,2,18], Andrew Dhawan[1,2,5,18,19], Scott J. Cameron[1,7,8], Justin D. Lathia[1,2,5,6,19]

[1]Department of Cardiovascular & Metabolic Sciences, Lerner Research Institute, Cleveland Clinic, Cleveland, Ohio, USA

[2]Case Comprehensive Cancer Center, Cleveland, Ohio, USA

[3]Section on Clinical Genomics and Experimental Therapeutics, National Institute on Alcohol Abuse and Alcoholism, National Institutes of Health, Bethesda, Maryland, USA

[4]NIH Oxford-Cambridge Scholars Program, National Institutes of Health, Bethesda, Maryland, USA

[5]Cleveland Clinic Lerner College of Medicine of Case Western Reserve University, Cleveland, Ohio, USA

[6]Center for Immunotherapy and Precision Immuno-Oncology, Cleveland Clinic, Cleveland, Ohio, USA

[7]Department of Cardiovascular Medicine, Section of Vascular Medicine, Cleveland Clinic, Cleveland, Ohio, USA

[8]Heart Vascular and Thoracic Institute, Department of Cardiovascular Medicine, Section of Vascular Medicine, Cleveland Clinic, Cleveland, Ohio, USA

[9]Departments of Pathology and Neurological Surgery, Lou and Jean Malnati Brain Tumor Institute, Feinberg School of Medicine, Northwestern University, Chicago, Illinois.

[10]Neuroscience Institute and Department of Neurosurgery, Wright State University School of Medicine, Dayton, Ohio, USA

[11]Departments of Biochemistry, [15]Medicine, Hematology and Oncology Division, and [17]Pharmacology, Case Western Reserve University School of Medicine, Cleveland, Ohio, USA

[12]Department of Surgery, Washington University School of Medicine, St. Louis, Missouri, USA

[13]Department of Pediatrics, Washington University School of Medicine, St. Louis, Missouri, USA

[14]Department of Neurosciences, Washington University School of Medicine, St. Louis, Missouri, USA

[16]Medicine Service, Section of Hematology-Oncology, Louis Stokes Veterans, Cleveland, Ohio, USA

[18]Taussig Cancer Institute, Cleveland Clinic, Cleveland, Ohio, USA

[19]Rose Ella Burkhardt Brain Tumor & Neuro-Oncology Center, Cleveland Clinic, Cleveland, Ohio, USA

Corresponding author
Justin D. Lathia
9500 Euclid Ave, NE3-202
Cleveland, OH 44195
Phone: (216) 445-7475
E-mail: lathiaj@ccf.org

Figures: 5

Abstract:

Sex differences in cancer outcomes, including glioblastoma (GBM), are shaped by biological, hormonal, and immune factors, influencing disease progression, treatment responses, survival, and the tumor microenvironment (TME). Platelets, as key regulators of immune responses and tumor progression, may contribute to these sex-based differences by influencing the dynamics of the TME, however, the precise molecular mechanisms remain unclear. Here, we show that GBM patients exhibit heightened platelet reactivity driven by protease-activated receptor 4 (PAR4) signaling. In murine GBM models, targeting PAR4 with BMS986120 prolongs survival in females but not males. This survival advantage is estrogen-dependent and TME-specific, driven by enhanced CD8+ T cell infiltration within the tumor. Inhibiting platelet PAR4 signaling decreases platelet alpha-granule secretion in female tumor-bearing mice while enriching alternative exocytosis pathways, thereby influencing CD8+ T cell activity. PAR4-activated platelets within the TME suppress CD8+ T cell function and CD8+ T cell depletion eliminates the tumor induced platelet reactivity and survival benefit when PAR4 is inhibited. These findings establish platelet-mediated PAR4 signaling as a critical driver of tumor progression and identify sex-specific immune responses as key to therapeutic efficacy.

68 **Introduction**

69 Sex differences in cancer strongly underlie and influence risk, progression, and treatment outcomes. For
70 example, men are more likely to develop several cancer types, including glioblastoma (GBM), while women often
71 exhibit better survival rates. Despite these appreciated epidemiological differences, treatment paradigms remain
72 uniform, highlighting the opportunity for sex-specific therapies shaped by hormonal, genetic, and immune
73 differences. Sex differences in cancer also involves the tumor microenvironment (TME) — a complex network of
74 cells and anatomical structures, including blood vessels, that interact with tumors. Among the components of the
75 TME, platelets play a major role in maintaining vascular integrity and modulating immune responses, offering
76 key insights into the relationship between sex differences and cancer progression. While platelets are present in
77 the TME and known to influence immune cells, their role in cancer, particularly in thrombotic events and sex
78 differences via thrombin-PAR4 signaling, remains underexplored[1-4]. In a recent study, the antiplatelet drug
79 aspirin, which inhibits cyclooxygenase-1, enhanced the protective mechanism of T cells and therefore inhibited
80 metastasis in murine models of malignancy, further suggesting that platelets play a role in mediating cancer
81 progression[5].

82 In glioblastoma (GBM), the most common primary malignant brain tumor in adults, immune cells in the
83 TME suppress anti-tumor responses. Myeloid cells drive immune suppression in GBM, while lymphocytes, such
84 as CD8+ T cells, are reduced[6-8]. Moreover, GBM has a striking difference in incidence, with men 1.6 times more
85 likely to develop the disease and exhibiting shorter survival[9, 10]. Both intrinsic factors and immune cells such as
86 microglia, myeloid-derived suppressor cells (MDSCs), and CD8+ T cells contribute to these differences[6, 8], with
87 myeloid-derived cells having enhanced proliferation in males and male CD8+ T cells showing a greater
88 propensity for exhaustion. Although platelet-derived factors promote tumor growth, their underlying mechanisms
89 and role in sex-based differences in GBM are unclear[2, 11]. Thrombotic events, such as deep vein thrombosis
90 (DVT) and pulmonary embolism (PE), are common in cancer patients and a leading cause of morbidity and
91 mortality, despite the cause of death not being attributed to intravascular thrombosis[12, 13]. GBM patients face a
92 15-24% risk of thrombotic events, and patients with thrombotic events have worse outcomes, suggesting that a
93 pro-thrombotic state drives cancer progression[14-17]. Therefore, given the sex differences in the incidence and
94 aggressiveness of GBM that is driven by an immunosuppressive microenvironment more pronounced in males,

95 we sought to determine whether sex-dependent platelet effects contribute to the immunosuppressive TME in
96 GBM.

97 **Results**

98 **GBM patients have hyperactive platelets via PAR4 signaling**

99 The GBM TME shapes the trajectory of tumor growth and response to therapies. A variety of mechanisms
100 underlie TME-tumor interactions[18]; however, the role of the platelet is underappreciated. We and others have
101 previously reported that high platelet counts are temporally related to worsened clinical outcomes in patients with
102 any malignancy, including GBM[2, 19, 20]. By carefully evaluating the platelet transcriptome in the context of large-
103 scale datasets, we found that high platelet gene signatures are associated with poor overall survival in GBM
104 patients (**Figure 1A, Figure S1A**) and negatively correlated with several anti-tumor immune cell populations
105 including T cells, dendritic cells (DCs), and B cells (**Figure S1B**). This indicates that platelets are a negative
106 prognostic and immunosuppressive factor in GBM patients.

107 Next, we asked whether GBM patients have altered platelet physiology when compared to age- and sex
108 -matched control subjects. We measured platelet reactivity from peripheral blood using assays that measure
109 degranulation of platelet contents in GBM patients and control subjects. GBM patient platelets had increased
110 agonist-induced reactivity due to protease-activated receptor 4 (PAR4) signaling (**Figure S1B**). However,
111 agonist-induced platelet reactivity via protease-activated receptor 1 (PAR1), thromboxane receptor (TXA2), and
112 purinergic receptor P2Y12 were similar between GBM and control subjects (**Figure S2A-D**). Thrombin is a potent
113 human platelet agonist that acts via the PAR1 and PAR4 receptors and is quantified by measuring plasma levels
114 of the thrombin-antithrombin (TAT) complex in GBM patients. We found that GBM patients had significantly
115 higher levels of TAT relative to healthy age-matched control subjects (**Figure S1C**). Consistently, *in vivo* studies
116 utilizing murine GBM models demonstrated that tumor-bearing mice had increased platelet reactivity compared
117 to their baseline pre-tumor state (**Figure S1D, E**). Likewise, across patients with GBM, Mendelian randomization
118 analysis determined PAR4 expression to be predictive of GBM diagnosis, whereas other platelet receptor
119 expression was non-predictive (**Figure S3A-C**). This observation is consistent with previous reports indicating
120 agonist-induced platelet activation and spontaneous platelet activation were both increased in patients with late-
121 stage metastatic cancer[21] and further suggest that tumor-induced platelet reactivity is mediated by PAR4.

122 **Targeting the thrombin-PAR4 signaling axis prolongs survival in a female-specific manner**

123 To investigate the role of platelets in GBM tumor progression, C57BL/6 mice were intracranially
124 transplanted with murine GBM models followed by subsequent depletion of platelets through intravenous
125 administration of an anti-glycoprotein 1b (GP1b) antibody and survival analysis. These proof-of-concept studies
126 demonstrated that platelet depletion prolongs survival in female tumor-bearing mice. Inhibition of platelets had
127 no effect in male mice in both tumor models (**Figure 2A-B, Figure S4A-B**) despite similar levels of platelet
128 depletion (**Figure 2C, Figure S4C**). These results indicate that platelets drive tumor growth in a sex-biased
129 manner, prompting us to question whether targeting the enhanced PAR4-mediated platelet reactivity may also
130 show a sex difference in survival benefit.

131 We again transplanted C57BL/6 mice with murine GBM models and pharmacologically targeted the major
132 platelet PAR receptor in mice (PAR4) with daily treatment of the PAR4 antagonist BMS986120 via oral gavage.
133 Targeting PAR4 in tumor-bearing mice prolonged survival in a sex-dependent manner, with marked survival in
134 females and no impact in males in all three murine GBM models (**Figure 2D-G**, **Figure 5A, B**). To determine
135 whether these effects were due to higher PAR4 expression in females, we examined intratumoral PAR4 (F2RL3)
136 expression in GBM patient samples (TCGA) and found no difference in expression between tumors from males
137 and those from females (**Figure S5C**). These studies suggest that targeting PAR4 results in prolonged survival
138 in a sex-dependent manner. To ascertain whether effects observed were specific to PAR4 and not an off-target
139 effect of BMS986120, we transplanted tumor cells into PAR4-P310L transgenic animals, which have a 70%
140 reduction in PAR4 function[22]. Consistently, we observed that female PAR4-P310L mice had a longer survival
141 when compared with wildtype animals, whereas we observed no difference in male PAR4-P310L mice (**Figure**
142 **2H, I**).

143 We next investigated whether the prolonged survival observed in female mice may be due to the impact
144 of sex hormones. Based on the prediction that an estrogen response element is present on the PAR4 promoter,
145 we performed ovariectomies on female mice. One month later, we intracranially implanted GBM cells and
146 administered BMS986120. Estrogen depletion rescued any prior survival benefit observed with BMS986120
147 administration compared to sham-operation control mice (**Figure 2J**). These findings suggest that the survival
148 benefit of targeting PAR4 signaling in females is, at least in part, driven by estrogen, establishing a novel
149 connection between sex hormones and platelet-mediated tumor progression that underpins therapeutic
150 outcomes.

151 **Targeting thrombin-PAR4 signaling enhances CD8+ T cells in a sex-dependent manner**

152 Next, we sought to determine the mechanism by which targeting the thrombin-PAR4 signaling axis
153 prolongs survival in a sex-dependent manner. To determine whether the effect of BMS986120 was tumor cell
154 intrinsic, we assessed proliferation in multiple murine GBM cell models treated with BMS986120 and observed
155 no major differences in *in vitro* proliferation (**Figure S5D-F**), suggesting no significant impact on tumor cell fitness
156 with BMS986120 treatment. These results led us to test whether the survival benefit seen in female tumor-
157 bearing mice requires a fully functioning immune system. We intracranially transplanted NOD *scid* gamma (NSG)
158 mice with murine GBM cells and subsequently targeted PAR4 with BMS986120 administration.
159 Pharmacologically targeting PAR4 with BMS986120 in immune-incompetent mice did not show the survival
160 benefit observed in immune-competent models (**Figure 3A, B, Figure S5G, H**). These findings reveal that the
161 survival advantage seen in females when inhibiting the thrombin-PAR4 signaling axis depends on a functional
162 immune system.

163 Platelets are known to influence immune cell function within the TME and in the systemic circulation[23-27].
164 While heterologous cell interactions are known to impact GBM, the question of whether platelets have sex-
165 dependent effects is unexplored, and no studies have examined how PAR4 signaling regulates the TME across
166 malignancies. To determine how the thrombin-PAR4 signaling axis contributes to the TME, we conducted
167 immune profiling on tumor-infiltrating immune cells. We found that BMS986120-treated female mice had an
168 increased percentage of CD45hi/CD3+ cells, specifically CD45hi/CD8+ tumor-infiltrating T cells (**Figure 3B, C**
169 **Figure S6**), as well as an increase in cytokine expression upon ex vivo stimulation (**Figure 3D**). There were no
170 differences in other TME immune cell subsets (**Figure S7S-F, Figure S8A-F**).

171 To further validate that the female survival benefit was CD8+ T cell dependent, we intracranially
172 transplanted GBM cells in Rag1-/- mice, which lack T and B cells, and treated with BMS986120. Removing T
173 cells reverses the survival benefit observed when mice were treated with BMS981260 (**Figure 3E**). To isolate
174 the effect specifically to CD8+ T cells, we intracranially implanted murine GBM cells into C57BL/6 mice and
175 administered anti-CD8 depletion antibody in combination with BMS986120. These experiments revealed that
176 depleting CD8+ T cells in the presence of BMS986120 completely rescued the female survival benefit observed
177 when the thrombin-PAR 4 signaling axis was targeted (**Figure 3F, G**). Taken together, our results suggest that
178 the survival benefit of targeting thrombin-PAR4 signaling in GBM is sex dependent, driven by sex hormones, and

179 mediated through platelet interactions with CD8+ T cells in the TME, highlighting a unique platelet-immune
180 mechanism underlying therapeutic outcome.

181 **Targeting PAR4 enhances platelet secretion and exocytosis in a sex-dependent manner**

182 PAR receptors, including PAR4, are thought to be expressed on endothelial cells and T cells[28], implicating
183 two potential mechanisms that could occur when PAR4 is targeted: a direct enhancement of CD8+ T cells in
184 females or the inhibition of PAR4 signaling on platelets, which then indirectly enhances CD8+ T cell activity in
185 females. To this end, we explored PAR expression in human and mouse T cells by utilizing publicly available
186 datasets. We found that PAR4 was not expressed on T cells from mouse (**Figure S9A-D)** or human (**Figure**
187 **S10A-D)**. However, mouse (**Figure S9A-D)** and human (**Figure S10A-D**) T cells did express high levels of PAR1.
188 These results suggest that the increased tumor-infiltrating CD8+ T cells observed when targeting PAR4 in
189 females is platelet dependent and that platelet signaling likely regulates tumor-infiltrating CD8+ T cells in a sex-
190 dependent manner via PAR4.

191 We next determined how the pharmacological targeting of platelet PAR4 signaling alters platelet function
192 and signaling in tumor-bearing mice. We intracranially transplanted GBM cells and treated mice with BMS986120
193 for 14 days. Aggregation assays demonstrated that pharmacologically targeting PAR4 for 14 days had no effect
194 on aggregation/thrombosis in tumor-bearing mice (**Figure 4A**). However, flow cytometry for CD62P on platelets
195 showed that female tumor-bearing mice had inhibited regulated alpha granule secretion following a 14-day
196 treatment with BMS986120 (**Figure 4B, D**), whereas the male mice treated with BMS986120 had no change in
197 alpha granule secretion (**Figure 4C, E**). Proteomic GO enrichment analysis demonstrated that peripheral
198 platelets from BMS986120-treated female mice had enriched platelet degranulation and exocytosis signaling
199 pathways (**Figure 4F**). These results suggest that inhibiting alpha-granule secretion yet stimulating other
200 exocytosis and secretion mechanisms (i.e., dense granule secretion and Weibel Palade bodies) may regulate
201 tumor infiltrating CD8+ T cells in a sex-dependent manner.

202 **Bidirectional regulation of functions between platelets and CD8+ T cells**

203 This and previous work has demonstrated that high platelet counts associate with poor survival in GBM
204 and multiple other malignancies[2, 29-32]. Platelets also interact with and educate the function of other cells including
205 immune cells that have been identified in the TME and within the circulation[23-27], however the role of platelets in
206 regulating the immunosuppressive tumor microenvironment remains poorly understood. When CD8+ T cells

were co-cultured with fresh platelets daily, T cell function as measured by intracellular cytokine expression (**Figure 5A, B**) and cytokine secretion (**Figure 5C, D**), were inhibited. This effect could be reversed with BMS986120 treatment of T cells and platelets isolated from female mice but not males (**Figure 5C, D**). In a *in vivo* setting, GBM tumor-bearing immunocompetent mice have constitutively higher platelet reactivity relative to their baseline. However, platelet hyperreactivity is not observed in tumor-bearing NSG mice which lack T, B, and NK cells (**Figure S10**). To further decipher whether tumor-induced platelet reactivity is T cell specific, GBM tumors were induced in RAG1$^{-/-}$ mice which have no B or T cells. In this case, no increase in platelet reactivity was observed (**Figure 5E**). Consistently, we also tested platelet activity in tumor-bearing mice that were pretreated with an anti-CD8 antibody, wherein no enhanced platelet reactivity was found (**Figure 5F**). These results reveal that tumor-induced platelet reactivity in murine glioblastoma (GBM) models is dependent on the presence of immune cells, particularly CD8+ T cells (**Figure 5G**). GBM models is dependent on the presence of immune cells, particularly CD8+ T cells (**Figure 5G**).

Discussion

Our study identifies, for the first time, a novel connection among platelet signaling, hormonal regulation, and immune activity within the GBM TME. We show that PAR4 inhibition selectively enhances survival in female tumor-bearing mice by modulating platelet-driven immune suppression, with no effect in males. Mechanistic studies revealed that this sex-specific response is linked to platelet secretion and exocytosis pathways influenced by estrogen. Upon tumor formation, platelet reactivity and thrombotic markers highlight a pro-thrombotic state that drives immune suppression and disease progression (**Fig. 5G**). Importantly, the sex-dependent effects of PAR4 inhibition suggest an interplay between thrombosis and hormonal regulation that could shape therapeutic outcomes. We demonstrate that targeting platelet PAR4 signaling enhances immune activation and survival in females. This is achieved through an altered TME-tumor immune function, which has been shown to have a sex bias in immune cell subpopulations such as microglia, MDSCs, and T cells [6-8]. This study highlights cancer-associated thrombosis as a key driver of tumor progression, supporting precision medicine strategies that account for sex as a biological variable.

Cancer patients have a significantly higher risk of developing thrombotic events compared to the general population, with an estimated ninefold increase in VTE risk[12, 13, 33, 34]. Recent studies highlight the role of platelet activation in the TME, influencing immune responses and promoting pro-thrombotic conditions[5]. Our work

235 expands on this concept by demonstrating that tumor formation heightens platelet reactivity through an additional
236 platelet receptor, PAR4, which directly contributes to immune suppression in a sex-dependent manner. This
237 underscores how tumors hijack normal physiological processes to create a microenvironment that supports their
238 progression and survival. Our findings emphasize the need to target cancer-associated thrombosis and platelet
239 activation as a therapeutic approach, paving the way for innovative strategies that integrate anticoagulation and
240 immune modulation in precision oncology to reduce risk of cancer-associated mortality.

241 Targeting PAR4 offers a therapeutic advantage over targeting PAR1 due to its distinct signaling kinetics,
242 which reduce bleeding risks while still effectively modulating platelet activity[22, 35, 36]. Unlike PAR1, which responds
243 rapidly to low thrombin concentrations, PAR4 requires higher thrombin levels for activation, leading to more
244 highly controlled platelet responses and minimizing excessive bleeding complications. Additionally, PAR4
245 mediates the prolonged signaling necessary for stable thrombus formation, whereas PAR1 activation results in
246 a rapid, transient signal. By selectively inhibiting PAR4, therapeutic strategies can limit thrombosis while
247 preserving essential hemostatic functions, reducing the likelihood of severe bleeding events associated with
248 PAR1 inhibition[22]. Previous work has demonstrated that inhibiting PAR4 enhances CD4+ T regulatory cells,
249 contributing to immunosuppression[37]; however, our results show that PAR4 inhibition enhanced CD8+ T cell
250 function in a sex-dependent manner. This could be due to T cells in brain tumors often exhibit exhaustion,
251 immunosuppression, and altered metabolism, which weaken their ability to combat the tumor effectively[38].
252 Compared to other tumor types, T cells in brain tumors face heightened challenges due to the brain's unique
253 immune-privileged status and the suppressive tumor microenvironment, which includes factors like regulatory T
254 cells and tumor-associated macrophages[39]. These elements contribute to reduced T cell infiltration and impaired
255 antitumor responses. These findings highlight PAR4 as a more favorable target for platelet inhibition in cancer-
256 associated thrombosis and other thrombotic disorders in females.

257 While our findings establish the role of PAR4-mediated platelet signaling in GBM progression and its sex-
258 dependent therapeutic implications, several limitations remain. Translating results from murine models to human
259 patients requires further clinical validation across diverse genetic and tumor backgrounds. Additionally, while
260 estrogen contributes to the survival benefit of PAR4 inhibition, broader hormonal influences on platelet function
261 and immune modulation warrant further exploration. The therapeutic potential of BMS986120 is promising, but
262 the long-term efficacy, safety, and off-target effects must be assessed in preclinical and clinical models.

Based on our findings, future research should investigate alternative platelet secretion mechanisms in shaping immune responses, with proteomic analyses identifying sex-specific signaling pathways that influence treatment efficacy. Examining how estrogen affects platelet-driven TME dynamics may yield novel hormone-modulating strategies to complement PAR4-targeted therapies. Expanding these insights into human studies and developing biomarkers for platelet activity could better predict patient outcomes. Further investigation into the combination therapy with platelet and immune modulation and synergy could help refine personalized, sex-specific therapeutic strategies.

Materials and Methods

Cell models

The syngeneic mouse GBM cell line SB28 and KR158 were generously gifted by Dr. Hideho Okada (University of California San Francisco). The GL261 line was from the Developmental Therapeutics Program, NCI. All cell lines were routinely tested for *Mycoplasma* and were preemptively treated with 1:100 MycoRemoval Agent (MP Biomedicals) upon thawing. All cell lines used in these studies were maintained in complete RPMI 1640 (Media Preparation Core, Cleveland Clinic Lerner Research Institute) supplemented with 10% FBS (Thermo Fisher Scientific), 1% penicillin/streptomycin (Media Preparation Core, Cleveland Clinic Lerner Research Institute). All cell lines were maintained at 37°C and 5% CO_2 in a humidified incubator.

Mice

All animal experiments were performed in accordance with IACUC policies and guidelines and approved by the IACUC committee at Cleveland Clinic Lerner Research Institute. C57BL/6 (RRID:IMSR_JAX:0006641), RAG1$^{-/-}$ (B6.129S7-Rag1tm1Mom/J; RRID:IMSR_JAX:002216), and NOD.Cg-*Prkdc*^{scid} *Il2rg*^{tm1Wjl}/SzJ (NSG; RRID:IMSR_JAX:005557) were purchased from The Jackson Laboratory as required. PAR4-P310L were a generous gift from Dr. Marvin Nieman at Case Western Reserve University[22].

Intracranial tumor transplantation and treatments

For intracranial tumor implantation, 4- to 7-week-old mice were intracranially injected with 10,000 to 20,000 cells in 10 µL of RPMI-null media, 3 mm caudal to the coronal structure, 1.8 mm lateral to the sagittal suture at a 90° angle with the skull to a depth of 3.0 mm. Animals were monitored daily for neurological symptoms that include lethargy and hunched posture to qualify signs of tumor burden. In some experiments, male and female mice were treated with 2 mg/kg BMS986120 (MedChemExpress) or vehicle (8% DMSO) via oral gavage, daily, beginning 1-7 days post tumor implantation depending on the tumor latency of the model. In other experiments, to deplete CD8+ T cells, mice were intraperitoneally injected with an anti-CD8 antibody (Bio X Cell, Cat. #0061) or isotype control antibody (Bio X Cell, cat. #BE0090). Animals were administered 200 µg of antibody on day -1, followed by 100 µg every 5 days until humane endpoint was reached as previously described[8]. In other experiments, to deplete platelets, anti-GPIbα (EMFRET, Cat. R300) or anti-igG was administered intraperitoneally 1 day post tumor implantation to avoid hemorrhage at a concentration of 1 µg/g. Subsequent administration was done at a concentration of 0.5 µg/g every 5 days until humane endpoint was reached.

299 *Ovariectomy*

300 For oophorectomy procedures, 4- to 7-week-old female mice were deeply anesthetized, and a
301 longitudinal incision was made 0.5 cm above where the upper border line of the two hind limbs connect with the
302 back. The skin incision was pulled approximately 0.5 cm horizontally to the left or the right to visualize two soft,
303 white, shiny fat masses next to the lower pole of the kidneys. The left and right ovaries of the mouse are found
304 in the respective fat masses and were bi-laterally ovariectomized by cutting each side of the ovary and excising
305 with sterile surgical scissors, which results in little to no bleeding. After the muscle layer was closed with sutures
306 and the skin incision was sutured or stapled, the mice were placed in a heated chamber to recover. Mice in the
307 sham group also underwent a similar procedure as the ovariectomized group, except the ovaries were left intact
308 and only some adipose tissue near the ovaries was removed.

309 *Human platelet isolation and stimulation*

310 Human platelet isolation was conducted as previously described[40, 41]. In brief, whole blood was collected from
311 healthy donors into tubes containing 3.2% sodium citrate (BD Vacutainer) using a 21-gauge butterfly needle to
312 ensure minimal activation during collection. Platelet-rich plasma (PRP) was obtained by centrifuging the collected
313 blood at 200 x g for 15 minutes at room temperature, carefully avoiding the buffy coat. PRP was then subjected
314 to a second centrifugation at 200 x g for 15 minutes to further purify the sample. The resulting supernatant was
315 discarded, and the PRP was diluted 1:1 with Tyrodes buffer. Prostaglandin I2 (PGI2, 10 nM final concentration)
316 was added to prevent spontaneous platelet activation during the isolation process. The PRP-Tyrode's mixture
317 was centrifuged at 1,400 x g for 5 minutes to pellet the platelets, and the supernatant was removed. Washed
318 platelets were resuspended in Tyrode's buffer and diluted 1:10 to achieve a working platelet suspension. Fifty
319 million platelets per mL was used immediately for subsequent activation assays.

320 For platelet activation, aliquots of 100 μL of the platelet suspension were stimulated with increasing
321 concentrations of agonists targeting the PAR1 receptor (TRAP6), the thromboxane receptor (U46619), the
322 P2Y12 receptor (ADP), and PAR4 (AY-NH2). Agonist concentrations ranged from 0.01 μM to 20 μM for TRAP6,
323 U46619, and ADP, and from 0.05 μg/mL to 1 μg/mL for CRP. After a 15-minute stimulation at room temperature,
324 1 μL of P-selectin antibody (anti-CD62P, clone AK-4, eBioscience) conjugated to PE was added to each sample
325 and incubated in the dark for 30 minutes to prevent photobleaching.

326 Following antibody staining, 100 μL of 2% formalin was added to each sample to fix the platelets. Fixed
327 samples were stored at 4°C for no longer than 16 hours prior to analysis. Flow cytometry was performed on a
328 BD Accuri C6, and fluorescence was detected using the FL-2 channel (for PE-conjugated antibodies). Platelet
329 activation was quantified based on the surface expression of CD62P, with data analyzed using FlowJo software.

330 *Mouse platelet isolation and stimulation*

331 Whole blood was collected from C57BL/6 mice via retro-orbital bleeding using heparinized capillary
332 tubes. Blood was drawn into tubes containing heparin/Tyrode's solution (1000 U/mL heparin in Tyrode's buffer,
333 1:20 dilution). The collected blood was gently mixed by inverting the tube and processed immediately. PRP was
334 isolated by centrifuging the whole blood at 1000 RPM for 5 minutes at room temperature. Plasma was carefully
335 collected, avoiding red blood cells, and subjected to a second centrifugation at 1000 RPM for 5 minutes to
336 remove remaining blood cells. The PRP was then supplemented with 1 μM PGI2 to prevent platelet activation
337 during isolation. The platelet pellet was obtained by centrifuging PRP at 2700 RPM for 5 minutes, after which
338 the supernatant was discarded. Platelets were resuspended in Tyrode's buffer and pooled to achieve a final
339 concentration suitable for stimulation experiments. Platelets were aliquoted into 96-well plates at a concentration
340 of 100 μL per well for subsequent activation assays.

341 For platelet activation, 1 μL of each agonist (thrombin, U46619, ADP, convulxin) was added to the
342 platelets, with final concentrations ranging from 0.1 to 20 μM, depending on the agonist. Platelet stimulation was
343 carried out at room temperature for 10 minutes. After stimulation, 1 μL of FITC-conjugated anti-CD62P antibody
344 (clone RB40.34, BD Biosciences) was added to each sample, and the platelets were incubated in the dark for
345 an additional 10 minutes to prevent photobleaching.

346 Following staining, 100 μL of 2% formalin was added to fix the platelets, and samples were either
347 immediately analyzed by flow cytometry or stored at 4°C for up to 16 hours prior to analysis. Flow cytometry was
348 performed on a BD Accuri C6 cytometer, and data were collected for 10,000 events per sample. The expression
349 of P-selectin (CD62P) on the platelet surface was used as an indicator of platelet activation, and data analysis
350 was carried out using FlowJo software.

351 *Immunophenotyping by flow cytometry*

352 At the designated time points, tumor-bearing left hemispheres were enzymatically digested using
353 collagenase IV (Sigma) and DNase I (Sigma) to generate a single-cell suspension, a Percoll centrifugation step,

354 followed by filtration through a 40-μm strainer. Cells were first stained with LIVE/DEAD Fixable Stains (Thermo
355 Fisher) on ice for 15 minutes, washed with PBS, and resuspended in an Fc receptor blocker (Miltenyi Biotec)
356 diluted in PBS/2% BSA, followed by incubation on ice for 10 minutes. Surface staining was performed using
357 fluorochrome-conjugated antibodies diluted in brilliant buffer (BD Biosciences) at a concentration of 1:100 to
358 1:250, with a 30-minute incubation on ice. After a subsequent wash in PBS/2% BSA, cells were fixed overnight
359 using Foxp3/Transcription Factor Fixation Buffer (eBioscience).

360 For intracellular staining, antibodies were prepared in Foxp3/Transcription Factor Permeabilization Buffer
361 at 1:250 to 1:500 and incubated at room temperature for 45 minutes. To detect intracellular cytokines, cells were
362 stimulated in complete RPMI medium using a Cell Stimulation Cocktail with a protein transport inhibitor
363 (eBioscience) for 4 hours. Following stimulation, cells underwent the same staining procedures as described
364 above.

365 *In vitro CD8+ T cell culture*

366 CD8+ T cells were extracted from the splenocytes of C57BL/6 mice using a magnetic bead isolation kit
367 (STEMCELL Technologies), following established protocols. The cells were then maintained in complete RPMI
368 medium supplemented with recombinant human IL-2 (30 U/mL, PeproTech) and activated using anti-CD3/anti-
369 CD28 Dynabeads (Invitrogen) at a bead-to-cell ratio of 1:10. In addition, platelets were isolated as previously
370 described and incorporated into the T cell culture for three consecutive days at a 1:1 ratio of CD8+ T cells to
371 platelets. Cells subsequently underwent the same staining procedures outlined above.

372 *Analysis of previously published scRNA-seq data*

373 *Patient samples and datasets*

374 This study utilized WHO grade 4 IDH wildtype GBM samples from four publicly available datasets: The Cancer
375 Genome Atlas (TCGA), Chinese Glioma Genome Atlas (CGGA_325, CGGA_893), and Glioma Longitudinal
376 Analysis (GLASS).

377 *Immune Cell Profiling*

378 The relative abundance of 22 immune cell subtypes within each tumor sample from each dataset was estimated
379 using CIBERSORTx with default parameters and the LM22 signature gene set. Additionally, a gene signature
380 for platelet expression (REACTOME_RESPONSE_TO_ELEVATED_PLATELET_CYTOSOLIC_CA2, MSigDB)
381 was scored for each sample using single sample gene set enrichment analysis (ssGSEA).

382 *Univariate survival analysis*

383 To evaluate the prognostic significance of immune cell infiltration, univariate Cox proportional hazards models
384 were constructed for each estimated immune cell population (including the Platelet Sig score) within each
385 dataset. Immune cell proportions and platelet signature score were z-score normalized and centered prior to
386 hazard ratio computation. Immune cell abundance and platelet signature score (platelet_sig) were dichotomized
387 at the median value for each cell type within each respective dataset. The resulting hazard ratios (HRs) for overall
388 survival are presented, with error bars indicating the 95% confidence intervals.

389 *Immune cell correlation analysis*

390 Spearman correlation coefficients between the estimated abundances of the major immune cell types and
391 platelet gene signature score were computed. Correlation coefficients were computed for each of the major
392 immune cell subtypes (B Cells, Dendritic Cells (DC), T Cells, NK Cells, Mast Cells, Microglia, Monocytes, and
393 Macrophages) within each dataset (CGGA_325, GLASS, TCGA).

394 *PAR4 expression analysis in cell subtypes*

395 To investigate the expression profile of the PAR4 gene (also known as F2RL3) across different cell populations
396 within the GBM TME, we analyzed single-cell RNA sequencing data from the GBMap dataset. The expression
397 level of PAR4 was assessed for various identified cell subtypes as previously annotated. A dot plot (Seurat v5)
398 was generated to visualize the results.

399 Mendelian Randomization Analysis

400 The European Ancestry consortium was used for this analysis. Genetic variants (G), typically single nucleotide
401 polymorphisms (SNPs), serve as instrumental variables (IVs) to assess the causal effect of an exposure (X; e.g.,
402 platelet count) on an outcome (Y; e.g., glioma risk). For the causal inference to be valid, three key assumptions
403 must be satisfied: IV1 (Relevance) — the genetic instruments must be robustly associated with the exposure,
404 typically derived from genome-wide association studies (GWAS); IV2 (Independence) — the genetic instruments
405 must not be associated with confounding variables (U) that jointly influence both the exposure and the outcome;
406 and IV3 (Exclusion Restriction) — the instruments must affect the outcome solely through the exposure and not
407 via any alternative biological pathways. The DAG visualizes how genetic variants influence the outcome only via
408 their effect on the exposure, assuming no horizontal pleiotropy or confounding from unmeasured variables.

409 *Code and data availability*

410 All data used for the above analyses are publicly available through the TCGA, CGGA, GLASS, and GBMap
411 datasets, including clinical and cell type metadata. Immune cell signatures are available through CIBERSORTx,
412 and the platelet gene signature is available through MSigDB. All analyses were performed in R version 4.3.0,
413 and all code to reproducibly perform these analyses will be provided on Github.

414 *Statistical analysis*

415 Data visualization and statistical analysis were conducted using GraphPad Prism (Version 9, GraphPad
416 Software Inc., RRID:SCR_002798). Depending on the dataset, unpaired or paired t-tests, as well as one-way or
417 two-way analysis of variance (ANOVA) with multiple comparison adjustments, were applied as described in the
418 figure legends. Survival analysis was evaluated using the log-rank test. For all analysis, statistical significance
419 was set at $P < 0.05$.

420 **Data Availability**

421 All data generated in this study are available upon request from the corresponding author, Dr. Justin D. Lathia
422 (lathiaj@ccf.org).

423 **Ethics Declaration**

424 *Competing interests*

425 Authors declare no competing interest.

426 **Code availability**

427 All code to reproducibly perform these analyses will be provided on Github. Additionally, all code used in this
428 study are available upon request from the corresponding author, Dr. Justin D. Lathia (lathiaj@ccf.org).

429 **Authors Contributions**

430 Conception and design: A.R.S, S.J.C, J.D.L

431 Development of methodology: A.R.S, G.B, A.A, J.L

432 Acquisition of data: A.R.S, G.B, D.R, T.J.A, I.J, L.T, T.N, N.R, G.P.T, A.V, X.Y, J.C, A.S, B. R., N.S., A.D

433 Analysis and interpretation of data: A.R.S, G.B, J. L

434 Writing review: A.R.S, J.L, E.M.H, J.D.R, S.J.C, J.D.L

435 Administrative, technical, or material support: C.N.H, A.E.S, J.B.R, C.G.H, E.S, F.W.L, T.A.C, A.K, M.N., A.D.

436 Study supervision: S.J.C, J.D.L.

Acknowledgements

We sincerely acknowledge the members of the Lathia laboratory for their valuable insights and constructive discussions. We are grateful for the illustrative contributions of Ms. Amanda Mendelsohn from Enterprise Creative at the Cleveland Clinic. We are grateful to Belinda Willard and her team at the Proteomics Core (Cleveland Clinic Lerner Research Institute). Additionally, we extend our gratitude to Drs. Matthew Flick and Silvio Antoniak (University of North Carolina Chapel Hill) for their support and constructive comments on the project. This work was supported by NIH grants NIH T32 CA059366 (A.R.S), F32 CA287655 (A.R.S), R35 NS127083 (J.D.L), P01 CA245705 (J.D.L, J.B.R), and HL158801 (SJC). This work as also supported by the Cleveland Clinic VeloSano Bike to Cure event (S.J.C and J.D.L) and the Midwest Brain Tumor Foundation (A.R.S). Dr. Khorana acknowledges research support from the National Heart, Lung and Blood Institute (U01HL143402; R01HL164516) and the Sondra and Stephen Hardis Chair in Oncology Research.

References

1. Aggarwal A, Jennings CL, Manning E, Cameron SJ. Platelets at the Vessel Wall in Non-Thrombotic Disease. Circ Res. 2023;132(6):775-90. Epub 20230316. doi: 10.1161/circresaha.122.321566. PubMed PMID: 36927182; PMCID: PMC10027394.
2. Sloan AR, Lee-Poturalski C, Hoffman HC, Harris PL, Elder TE, Richardson B, Kerstetter-Fogle A, Cioffi G, Schroer J, Desai A, Cameron M, Barnholtz-Sloan J, Rich J, Jankowsky E, Sen Gupta A, Sloan AE. Glioma stem cells activate platelets by plasma-independent thrombin production to promote glioblastoma tumorigenesis. Neuro-Oncology Advances. 2022;4(1). doi: 10.1093/noajnl/vdac172.
3. Liao K, Zhang X, Liu J, Teng F, He Y, Cheng J, Yang Q, Zhang W, Xie Y, Guo D, Cao G, Xu Y, Huang B, Wang X. The role of platelets in the regulation of tumor growth and metastasis: the mechanisms and targeted therapy. MedComm (2020). 2023;4(5):e350. Epub 20230914. doi: 10.1002/mco2.350. PubMed PMID: 37719444; PMCID: PMC10501337.
4. Sloan AR, Gordillo AJ, Kennemer A, Khorana AA, Horbinski C, Kaelber DC, Cameron SJ, Lathia JD. VTE incidence shortens survival in IDH-WT glioblastoma. medRxiv. 2025. Epub 20250109. doi: 10.1101/2025.01.08.25319908. PubMed PMID: 39830282; PMCID: PMC11741497.
5. Yang J, Yamashita-Kanemaru Y, Morris BI, Contursi A, Trajkovski D, Xu J, Patrascan I, Benson J, Evans AC, Conti AG, Al-Deka A, Dahmani L, Avdic-Belltheus A, Zhang B, Okkenhaug H, Whiteside SK, Imianowski CJ, Wesolowski AJ, Webb LV, Puccio S, Tacconelli S, Bruno A, Di Berardino S, De Michele A, Welch HCE, Yu IS, Lin SW, Mitra S, Lugli E, van der Weyden L, Okkenhaug K, Saeb-Parsy K, Patrignani P, Adams DJ, Roychoudhuri R. Aspirin prevents metastasis by limiting platelet TXA(2) suppression of T cell immunity. Nature. 2025. Epub 20250305. doi: 10.1038/s41586-025-08626-7. PubMed PMID: 40044852.
6. Turaga SM, Silver DJ, Bayik D, Paouri E, Peng S, Lauko A, Alban TJ, Borjini N, Stanko S, Naik UP, Keri RA, Connor JR, Barnholtz-Sloan JS, Rubin JB, Berens M, Davalos D, Lathia JD. JAM-A functions as a female microglial tumor suppressor in glioblastoma. Neuro Oncol. 2020;22(11):1591-601. doi: 10.1093/neuonc/noaa148. PubMed PMID: 32592484; PMCID: PMC7690368.
7. Bayik D, Zhou Y, Park C, Hong C, Vail D, Silver DJ, Lauko A, Roversi G, Watson DC, Lo A, Alban TJ, McGraw M, Sorensen M, Grabowski MM, Otvos B, Vogelbaum MA, Horbinski C, Kristensen BW, Khalil AM, Hwang TH, Ahluwalia MS, Cheng F, Lathia JD. Myeloid-Derived Suppressor Cell Subsets Drive Glioblastoma Growth in a Sex-Specific Manner. Cancer Discov. 2020;10(8):1210-25. Epub 20200416. doi: 10.1158/2159-8290.Cd-19-1355. PubMed PMID: 32300059; PMCID: PMC7415660.
8. Lee J, Nicosia M, Hong ES, Silver DJ, Li C, Bayik D, Watson DC, Lauko A, Kay KE, Wang SZ, Johnson S, McGraw M, Grabowski MM, Kish DD, Desai AB, Goodman WA, Cameron SJ, Okada H, Valujskikh A, Fairchild RL, Ahluwalia MS, Lathia JD. Sex-Biased T-cell Exhaustion Drives Differential Immune Responses in Glioblastoma. Cancer Discov. 2023;13(9):2090-105. doi: 10.1158/2159-8290.Cd-22-0869. PubMed PMID: 37378557; PMCID: PMC10481130.
9. Ostrom QT, Rubin JB, Lathia JD, Berens ME, Barnholtz-Sloan JS. Females have the survival advantage in glioblastoma. Neuro Oncol. 2018;20(4):576-7. doi: 10.1093/neuonc/noy002. PubMed PMID: 29474647; PMCID: PMC5909625.
10. Ostrom QT, Kinnersley B, Wrensch MR, Eckel-Passow JE, Armstrong G, Rice T, Chen Y, Wiencke JK, McCoy LS, Hansen HM, Amos CI, Bernstein JL, Claus EB, Il'yasova D, Johansen C, Lachance DH, Lai RK, Merrell RT, Olson SH, Sadetzki S, Schildkraut JM, Shete S, Rubin JB, Lathia JD, Berens ME, Andersson U, Rajaraman P, Chanock SJ, Linet MS, Wang Z, Yeager M, Houlston RS, Jenkins RB, Melin B, Bondy ML, Barnholtz-Sloan JS. Sex-specific glioma genome-wide association study identifies new risk locus at 3p21.31 in females, and finds sex-differences in risk at 8q24.21. Sci Rep. 2018;8(1):7352. Epub 20180509. doi: 10.1038/s41598-018-24580-z. PubMed PMID: 29743610; PMCID: PMC5943590.
11. Fomchenko EI, Holland EC. Platelet-derived growth factor-mediated gliomagenesis and brain tumor recruitment. Neurosurg Clin N Am. 2007;18(1):39-58, viii. Epub 2007/01/25. doi: 10.1016/j.nec.2006.10.006. PubMed PMID: 17244553.
12. Khorana AA, Mackman N, Falanga A, Pabinger I, Noble S, Ageno W, Moik F, Lee AYY. Cancer-associated venous thromboembolism. Nat Rev Dis Primers. 2022;8(1):11. Epub 20220217. doi: 10.1038/s41572-022-00336-y. PubMed PMID: 35177631.
13. Wang TF, Khorana AA, Agnelli G, Bloomfield D, Bonaca MP, Büller HR, Connors JM, Goto S, Jing ZC, Kakkar AK, Khder Y, Raskob GE, Soff GA, Verhamme P, Weitz JI, Carrier M. Treatment of Cancer-Associated Thrombosis: Recent Advances, Unmet Needs, and Future Direction. Oncologist. 2023;28(7):555-64. doi: 10.1093/oncolo/oyad116. PubMed PMID: 37171998; PMCID: PMC10322141.

14. Sloan AR, Gordillo AJ, Kennemer A, Khorana AA, Horbinski C, Kaelber DC, Cameron SJ, Lathia JD. Venous thromboembolism incidence shortens survival in isocitrate dehydrogenase wild-type glioblastoma. Neurooncol Adv. 2025;7(1):vdaf018. Epub 20250131. doi: 10.1093/noajnl/vdaf018. PubMed PMID: 40264942; PMCID: PMC12012773.
15. Burdett KB, Unruh D, Drumm M, Steffens A, Lamano J, Judkins J, Schwartz M, Javier R, Amidei C, Lipp ES, Peters KB, Lai A, Eldred BSC, Heimberger AB, McCortney K, Scholtens DM, Horbinski C. Determining venous thromboembolism risk in patients with adult-type diffuse glioma. Blood. 2023;141(11):1322-36. doi: 10.1182/blood.2022017858. PubMed PMID: 36399711; PMCID: PMC10082363.
16. Diaz M, Jo J, Smolkin M, Ratcliffe SJ, Schiff D. Risk of Venous Thromboembolism in Grade II-IV Gliomas as a Function of Molecular Subtype. Neurology. 2021;96(7):e1063-e9. Epub 20201222. doi: 10.1212/wnl.0000000000011414. PubMed PMID: 33361259; PMCID: PMC8055337.
17. Unruh D, Horbinski C. Beyond thrombosis: the impact of tissue factor signaling in cancer. J Hematol Oncol. 2020;13(1):93. Epub 2020/07/16. doi: 10.1186/s13045-020-00932-z. PubMed PMID: 32665005; PMCID: PMC7362520.
18. Xiao T, Lee J, Gauntner TD, Velegraki M, Lathia JD, Li Z. Hallmarks of sex bias in immuno-oncology: mechanisms and therapeutic implications. Nat Rev Cancer. 2024;24(5):338-55. Epub 20240408. doi: 10.1038/s41568-024-00680-z. PubMed PMID: 38589557.
19. Suzuki K, Aiura K, Kitagou M, Hoshimoto S, Takahashi S, Ueda M, Kitajima M. Platelets counts closely correlate with the disease-free survival interval of pancreatic cancer patients. Hepatogastroenterology. 2004;51(57):847-53. Epub 2004/05/18. PubMed PMID: 15143932.
20. Lin MS, Huang JX, Zhu J, Shen HZ. Elevation of platelet count in patients with colorectal cancer predicts tendency to metastases and poor prognosis. Hepatogastroenterology. 2012;59(118):1687-90. Epub 2012/05/18. doi: 10.5754/hge12277. PubMed PMID: 22591645.
21. Cooke NM, Egan K, McFadden S, Grogan L, Breathnach OS, O'Leary J, Hennessy BT, Kenny D. Increased platelet reactivity in patients with late-stage metastatic cancer. Cancer Med. 2013;2(4):564-70. Epub 2013/10/25. doi: 10.1002/cam4.86. PubMed PMID: 24156029; PMCID: PMC3799291.
22. Han X, Knauss EA, Fuente M, Li W, Conlon RA, LePage DF, Jiang W, Renna SA, McKenzie SE, Nieman MT. A mouse model of the protease-activated receptor 4 Pro310Leu variant has reduced platelet reactivity. J Thromb Haemost. 2024;22(6):1715-26. Epub 20240319. doi: 10.1016/j.jtha.2024.03.004. PubMed PMID: 38508397.
23. In 't Veld S, Wurdinger T. Tumor-educated platelets. Blood. 2019;133(22):2359-64. Epub 2019/03/06. doi: 10.1182/blood-2018-12-852830. PubMed PMID: 30833413.
24. Verheul HM, Jorna AS, Hoekman K, Broxterman HJ, Gebbink MF, Pinedo HM. Vascular endothelial growth factor-stimulated endothelial cells promote adhesion and activation of platelets. Blood. 2000;96(13):4216-21. Epub 2000/12/09. PubMed PMID: 11110694.
25. Nash GF, Turner LF, Scully MF, Kakkar AK. Platelets and cancer. Lancet Oncol. 2002;3(7):425-30. Epub 2002/07/27. doi: 10.1016/s1470-2045(02)00789-1. PubMed PMID: 12142172.
26. Pinedo HM, Verheul HM, D'Amato RJ, Folkman J. Involvement of platelets in tumour angiogenesis? Lancet. 1998;352(9142):1775-7. Epub 1998/12/16. doi: 10.1016/s0140-6736(98)05095-8. PubMed PMID: 9848370.
27. Fomchenko EI, Holland EC. Platelet-derived growth factor-mediated gliomagenesis and brain tumor recruitment. Neurosurg Clin N Am. 2007;18(1):39-58, viii. PubMed PMID: 17244553.
28. Shpacovitch V, Feld M, Hollenberg MD, Luger TA, Steinhoff M. Role of protease-activated receptors in inflammatory responses, innate and adaptive immunity. J Leukoc Biol. 2008;83(6):1309-22. Epub 20080319. doi: 10.1189/jlb.0108001. PubMed PMID: 18347074.
29. Williams M, Liu ZW, Woolf D, Hargreaves S, Michalarea V, Menashy R, Kooner I, Wilson E. Change in platelet levels during radiotherapy with concurrent and adjuvant temozolomide for the treatment of glioblastoma: a novel prognostic factor for survival. J Cancer Res Clin Oncol. 2012;138(10):1683-8. Epub 2012/05/31. doi: 10.1007/s00432-012-1243-x. PubMed PMID: 22644996.
30. Takemoto A, Okitaka M, Takagi S, Takami M, Sato S, Nishio M, Okumura S, Fujita N. A critical role of platelet TGF-β release in podoplanin-mediated tumour invasion and metastasis. Sci Rep. 2017;7:42186. Epub 2017/02/09. doi: 10.1038/srep42186. PubMed PMID: 28176852; PMCID: PMC5297242.
31. Midorikawa Y, Takayama T, Higaki T, Aramaki O, Teramoto K, Yoshida N, Tsuji S, Kanda T, Moriyama M. High platelet count as a poor prognostic factor for liver cancer patients without cirrhosis. Biosci Trends. 2020;14(5):368-75. Epub 2020/07/28. doi: 10.5582/bst.2020.03230. PubMed PMID: 32713867.

32. Baranyai Z, Jósa V, Tóth A, Szilasi Z, Tihanyi B, Zaránd A, Harsanyi L, Szállási Z. Paraneoplastic thrombocytosis in gastrointestinal cancer. Platelets. 2016;27(4):269-75. Epub 2016/05/03. doi: 10.3109/09537104.2016.1170112. PubMed PMID: 27136385.
33. Wan T, Song J, Zhu D. Cancer-associated venous thromboembolism: a comprehensive review. Thrombosis Journal. 2025;23(1):35. doi: 10.1186/s12959-025-00719-7.
34. Wang TF, Li A, Garcia D. Managing thrombosis in cancer patients. Res Pract Thromb Haemost. 2018;2(3):429-38. Epub 2018/07/27. doi: 10.1002/rth2.12102. PubMed PMID: 30046747; PMCID: PMC6046582.
35. Künze G, Isermann B. Targeting biased signaling by PAR1: function and molecular mechanism of parmodulins. Blood. 2023;141(22):2675-84. doi: 10.1182/blood.2023019775. PubMed PMID: 36952648; PMCID: PMC10646804.
36. Li S, Wang W, Lin L, Yang L, Cai Y, Yang X, Zhang T, Xiao C, Yan H, Gao N, Zhao J. Oligosaccharide Blocks PAR1 (Proteinase-Activated Receptor 1)-PAR4-Mediated Platelet Activation by Binding to Thrombin Exosite II and Impairs Thrombosis. Arterioscler Thromb Vasc Biol. 2023;43(2):253-66. Epub 20221215. doi: 10.1161/atvbaha.122.318085. PubMed PMID: 36519467.
37. Bock M, Bergmann CB, Jung S, Biberthaler P, Heimann L, Hanschen M. Platelets differentially modulate CD4(+) Treg activation via GPIIa/IIIb-, fibrinogen-, and PAR4-dependent pathways. Immunol Res. 2022;70(2):185-96. Epub 20211221. doi: 10.1007/s12026-021-09258-5. PubMed PMID: 34932195; PMCID: PMC8917040.
38. Mohme M, Neidert MC. Tumor-Specific T Cell Activation in Malignant Brain Tumors. Front Immunol. 2020;11:205. Epub 20200213. doi: 10.3389/fimmu.2020.00205. PubMed PMID: 32117316; PMCID: PMC7031483.
39. Yang W, Liu S, Mao M, Gong Y, Li X, Lei T, Liu C, Wu S, Hu Q. T-cell infiltration and its regulatory mechanisms in cancers: insights at single-cell resolution. J Exp Clin Cancer Res. 2024;43(1):38. Epub 20240202. doi: 10.1186/s13046-024-02960-w. PubMed PMID: 38303018; PMCID: PMC10835979.
40. Morrell CN, Mix D, Aggarwal A, Bhandari R, Godwin M, Owens P, 3rd, Lyden SP, Doyle A, Krauel K, Rondina MT, Mohan A, Lowenstein CJ, Shim S, Stauffer S, Josyula VP, Ture SK, Yule DI, Wagner LE, 3rd, Ashton JM, Elbadawi A, Cameron SJ. Platelet olfactory receptor activation limits platelet reactivity and growth of aortic aneurysms. J Clin Invest. 2022;132(9). Epub 2022/03/25. doi: 10.1172/jci152373. PubMed PMID: 35324479; PMCID: PMC9057618.
41. Godwin MD, Aggarwal A, Hilt Z, Shah S, Gorski J, Cameron SJ. Sex-Dependent Effect of Platelet Nitric Oxide: Production and Platelet Reactivity in Healthy Individuals. JACC Basic Transl Sci. 2022;7(1):14-25. Epub 20211208. doi: 10.1016/j.jacbts.2021.10.009. PubMed PMID: 35128205; PMCID: PMC8807728.

611 **Figures and Figure Legends**

612 **Figure 1**

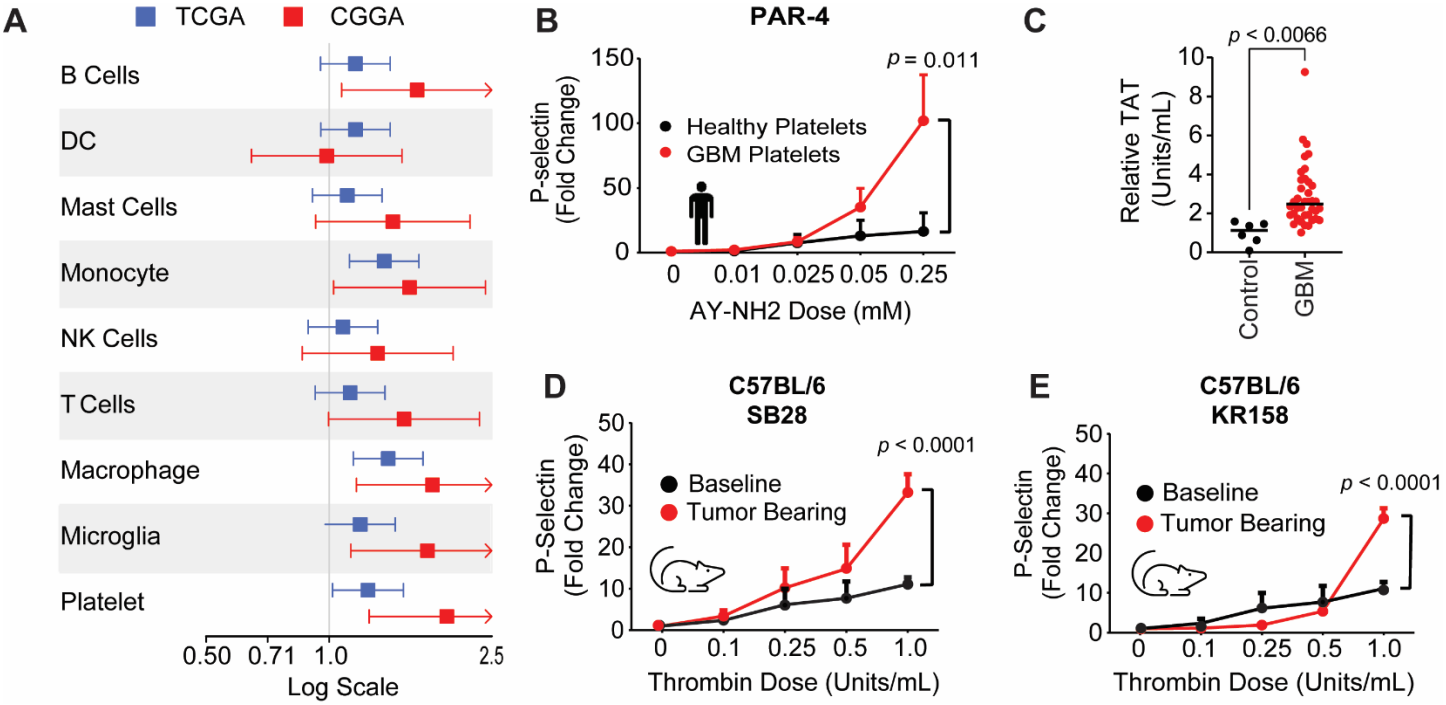

613

614 **Figure 1. GBM patients have hyperactive platelets via PAR4 signaling. A**. WHO grade 4 IDH wildtype GBM
615 samples from the publicly available data sets The Cancer Genome Atlas (TCGA) and Chinese Glioma Genome
616 Atlas (CGGA_325). Univariate Cox proportional hazards models were constructed, and deconvoluted immune
617 cell proportions and platelet signature score were z-score normalized and centered prior to hazard ratio
618 computation. Hazard ratios depicted describe overall survival with 95% confidence intervals as a function of
619 immune cell proportion or platelet signature score. **B**. Washed platelets isolated from patients with a GBM
620 diagnosis and matched control subjects were treated with AY-NH2 to stimulate PAR4, and α-granule secretion
621 was measured using an antibody specific for P-selectin via flow cytometry. Data are represented as means ±
622 SEM from *n*=18 GBM patients and *n*=13 control patients. Two-way ANOVA was performed. **C**. Thrombin-
623 antithrombin (TAT) expression in plasma from GBM and healthy patient platelets as measured by TAT ELISA.
624 An unpaired student's *t*-test was performed. (**D-E**) Washed platelets were isolated from mice before intracranial
625 tumor implantation (baseline) and following intracranial injection of the murine GBM SB28 (**D**) and KR158 (**E**).
626 Following tumor formation, washed platelets were isolated, and α-granule secretion was measured using an
627 antibody specific for P-selectin via flow cytometry. Data are represented as means ± SEM from n=4 independent
628 experiments. Two-way ANOVA was performed.

629

630

631

632

633

634

635

636

Figure 2

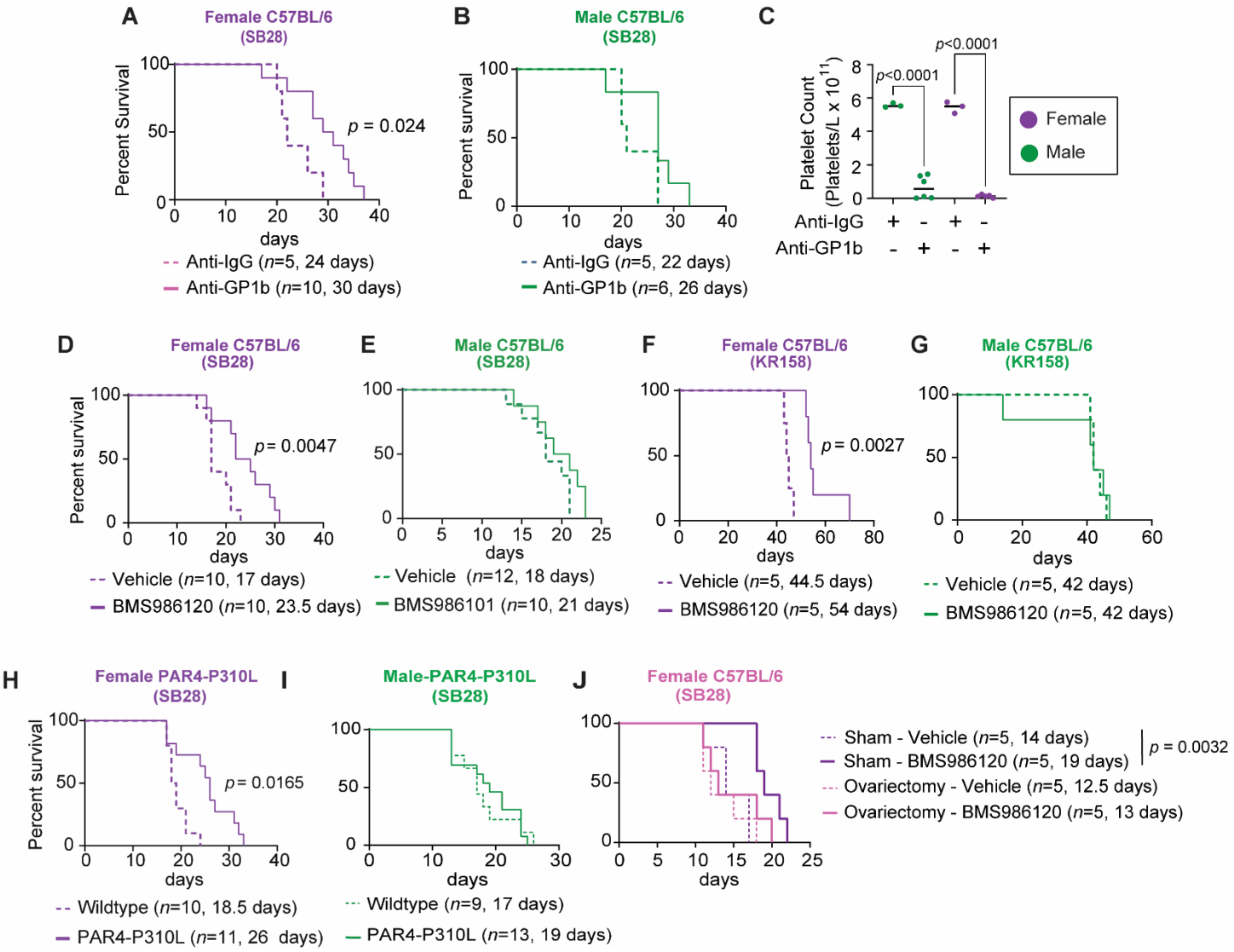

Figure 2. Targeting platelets via the thrombin-PAR4 signaling axis prolongs survival in a sex-dependent manner. A, **B**. Kaplan-Meier survival curves depicting survival of SB28 tumor-bearing female (**A**) and male (**B**) mice treated with anti-GP1bα depleting antibody. Statistical significance for survival analysis was determined by log-rank test. (**C**). Complete blood count (CBC) platelet reading 1 day post anti-GP1bα to validate platelet depletion in the tumor-bearing mice used in panels a and b. One-way ANOVA analysis with Tukey's multiple comparison test was performed. Kaplan-Meier survival analysis was performed after intracranial transplantation of the mouse GBM cell models SB28 (**D, E**) and KR158 (**F, G**) in immunocompetent C57BL/6 mice followed by pharmacologically targeting the thrombin-PAR4 signaling axis by administering BMS986120 (2 mg/kg), a selective PAR4 inhibitor. **H**, **I.** Kaplan-Meier survival analysis comparing male (**H**) and female (**I**) C57BL/6 wildtype and C57BL/6 - PAR-P310L mice following intracranial transplantation of the mouse GBM cell model SB28. **J**. Survival analysis of C57BL/6 female mice who underwent an ovariectomy or sham procedure and were intracranially transplanted with SB28 cells 30 days post ovariectomy and subsequently treated with BMS986120 (2 mg/kg). Statistical significance for survival analysis was determined by log-rank test.

Figure 3

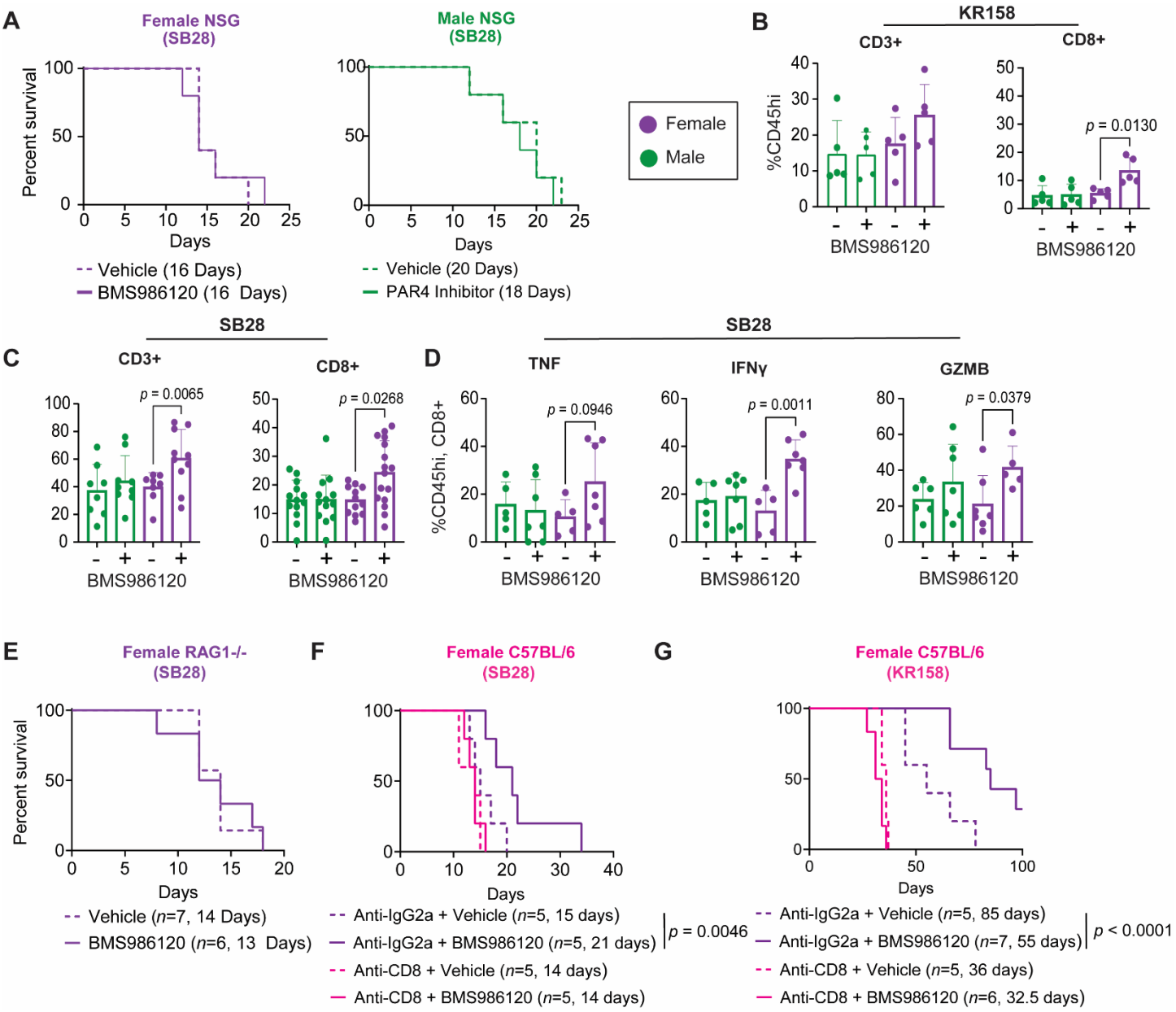

Figure 3. Targeting thrombin-PAR4 signaling enhances CD8+ T cells in a sex-dependent manner. Kaplan-Meier survival analysis was performed after intracranial injection of the mouse GBM cell model SB28 in immunodeficient NSG mice followed by pharmacologically targeting the thrombin-PAR4 signaling axis by administering BMS986120 (2 mg/kg), a selective PAR4 inhibitor (**A**). **B-C**. Frequency of tumor-infiltrating T-cell subsets 35 days post intracranial implantation of KR158 (**B**) and 14 days post intracranial implantation of SB28 (**C**) in male and female C57BL/6 mice treated with and without BMS986120. Data are combined from two independent experiments. One-way ANOVA analysis with Tukey's multiple comparison test was performed. **D**. Intracellular cytokine expression in tumor-infiltrating CD8+ T cells. Data are combined from two independent experiments. One-way ANOVA analysis with Tukey's multiple comparison test was performed. **E**. Kaplan-Meier survival curve depicting survival of SB28-bearing RAG1-/- female mice treated with BMS986120. **F-G**. Kaplan-Meier survival curves depicting survival of SB28 tumor-bearing female mice (**f**) and KR158 tumor-bearing female mice (**G**) treated with anti-CD8-depleting antibody with BMS986120 administration. Statistical significance for survival analysis was determined by log-rank test.

671 **Figure 4**

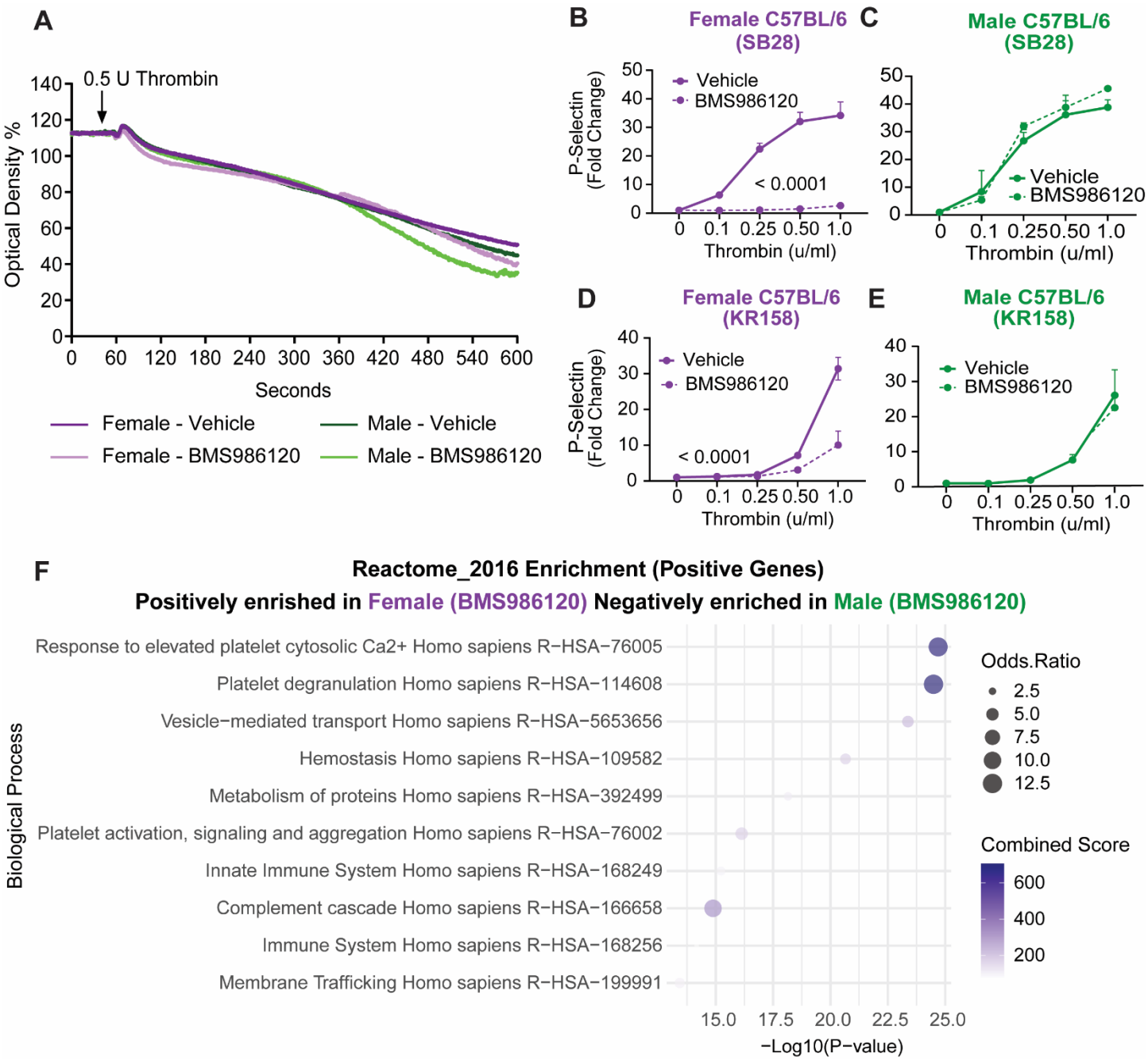

672

673 **Figure 4. Targeting PAR4 enhances platelet secretion and exocytosis in a sex-dependent manner. A.**
674 Aggregometry analysis of washed platelets isolated from mice treated with BMS986120 following intracranial
675 implantation of SB28 and stimulated with 0.5 U thrombin. Statistical significance was determined by a two-way
676 ANOVA. **B-E.** Washed platelets isolated from mice treated with BMS986120 following intracranial implantation
677 of SB28 (**B, C**) or KR158 (**D, E**). Washed platelets were isolated, and α-granule secretion was measured using
678 an antibody specific for P-selectin. Data are represented as means ± SEM. Statistical significance was
679 determined by two-way ANOVA. **F**. Proteomic GO enrichment analysis of washed platelets isolated from mice
680 treated with BMS986120 following intracranial implantation of SB28. Pathways are positively enriched in female
681 BMS986120 platelets and negatively enriched in male BMS986120 platelets.

682

683

Figure 5

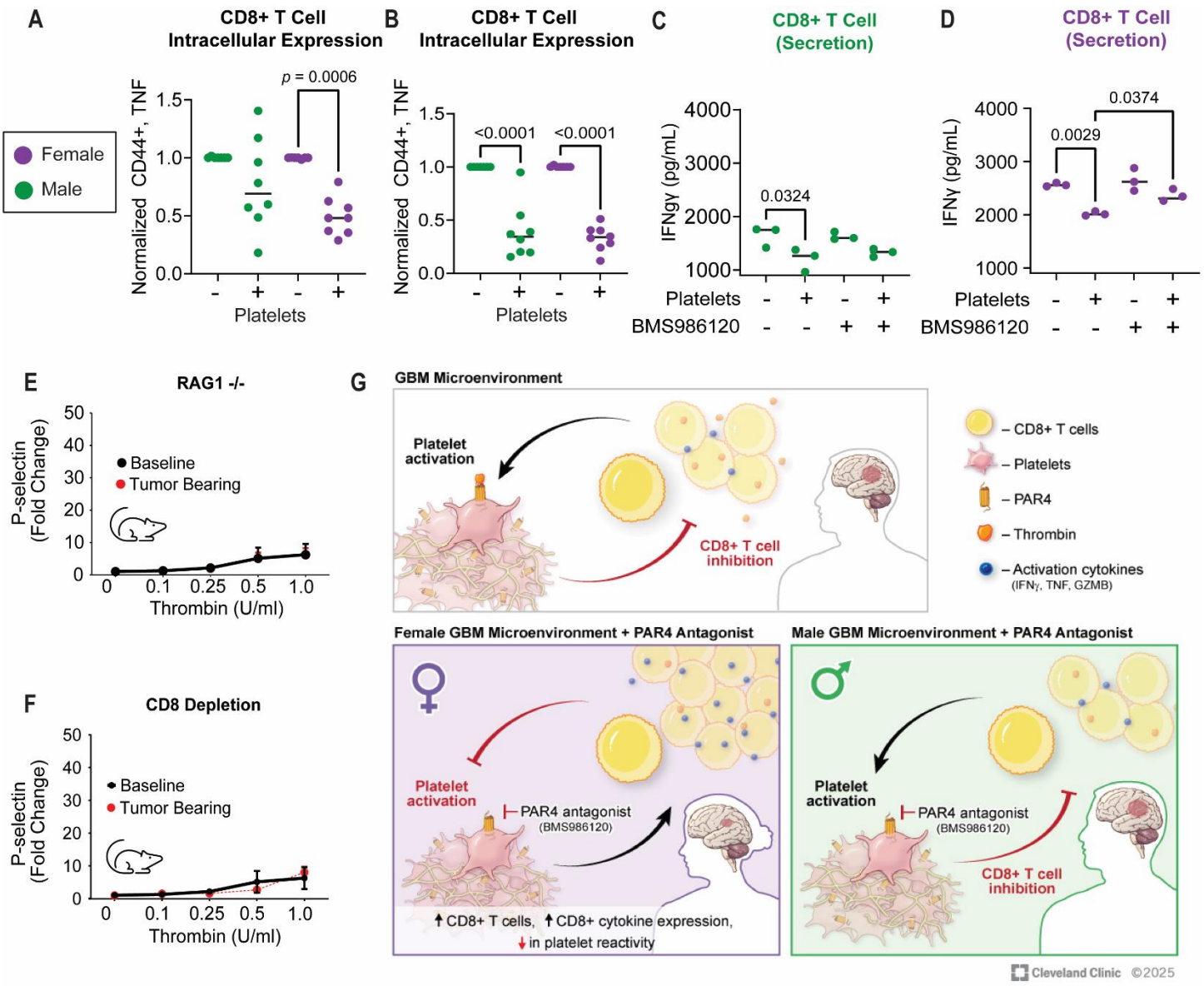

Figure 5. Bidirectional regulation between platelets and CD8+ T cells. A, B. Intracellular cytokine expression of CD8+ T cells isolated from C57BL/6 mouse spleen and co-cultured with sex-matched washed platelets isolated from B6 wildtype mice; fresh platelets were added for 3 consecutive days, and intracellular TNF (**A**) and IFNγ (**B**) expression was measured by flow cytometry. One-way ANOVA analysis with Tukey's multiple comparison test was performed. **C, D**. IFNγ cytokine secretion from male (**C**) and female (**D**) CD8+ T cells isolated from C57BL/6 mouse spleen and co-cultured with sex-matched washed platelets isolated from C57BL/6 mice; fresh platelets were added for 3 consecutive days, and supernatant IFNγ secretion was measured by ELISA. One-way ANOVA analysis with Tukey's multiple comparison test was performed. **E, F**. Washed platelets isolated from RAG1-/- mice (**C**) and C57BL/6-CD8-depleted mice (**D**) before intracranial tumor implantation (baseline) and two weeks following intracranial injection of SB28 cells. Washed platelets were isolated, and α-granule secretion was measured using an antibody specific to P-selectin via flow cytometry. Data are represented as means ± SEM from n=4 independent experiments. **G**. Proposed model suggesting platelet-mediated PAR4 signaling is as a critical driver of tumor progression and identifying sex-specific immune responses as key to therapeutic efficacy.